February 28, 2026

Jeonghoon Lee, Ph. D

Professor
Dept. of Science Education
Ewha Womans University
Seoul 120-750, Korea
Email: jeonghoon.d.lee@gmail.com
Tel: +82-2-3277-3794

Dear Editor Gabriele Messori,

We are pleased to submit the revised version of our manuscript entitled *"Climate-related signals in the GV7-C ice core from East Antarctica for 1782–2013 CE: Potential relevance to climate and teleconnections between tropics and Antarctica"* for consideration in **Earth System Dynamics**. We sincerely appreciate the constructive comments and insightful suggestions provided by you and the reviewers. We have carefully addressed all comments and believe that the manuscript has been substantially improved. Detailed responses are provided below.

Reply to the comments by reviewer #1

General comment: The manuscript by Nyamgerel et al investigates climate related signals in the GV7-C ice core located in East Antarctica, and the potential teleconnections between the tropics and Antarctica. While the manuscript addresses an important question regarding the climate variability signals within the GV7-C ice core in East Antarctica, major revisions are necessary before it can be considered for publication.

Answer: We sincerely appreciate the reviewer's thoughtful evaluation and constructive feedback. In response to the major revision request, we have carefully revised the manuscript, strengthened the methodological transparency, clarified the results, and improved the overall structure.

My main concerns that need to be addressed before further review are:

Comment 1: (1) Additional detail added to the method. Currently the method lacks sufficient detail to understand and have confidence in the results and interpretation. My key concerns include:

- No information is provided on important data processing and statistical information, including any detrending of dataset or consideration of how trends influence correlation results, statistical tests used for significance, consideration of autocorrelation and degrees of freedom on significance.

Answer: We sincerely appreciate the reviewer's comment highlighting the need for clearer statistical description and methodological transparency. In response, we have revised the entire Section 2.3 (Climate data and analysis) to explicitly describe data preprocessing and statistical procedures as following. Specifically, (a) All datasets used in the correlation analysis were linearly detrended prior to analysis; (b) Statistical significance of Pearson correlation coefficients was assessed using a two-tailed Student's *t*-test; and (c) The two time periods (1957–2013 CE and 1872–2013 CE) were selected based on data availability and to ensure sufficiently large sample sizes for more reliable comparison. We acknowledge that climatic and ice-core time series may exhibit serial autocorrelation, which can reduce the effective degrees of freedom and potentially inflate nominal significance levels. Although a formal calculation of effective degrees of freedom was not explicitly performed in this study, the strongest reported correlations (e.g., between d-excess and SST-SEIO in the smoothed time series) are sufficiently large in magnitude that even under conservative assumptions of reduced effective sample size, the significance and overall interpretation would not substantially change.

"The $\delta^{18}O$ ($\delta^{18}O$ preferred and the correlation with δD is 0.99), *d*-excess, and SA from the GV7-C ice core were used in the analysis. Two time periods (1957–2013 CE and 1872–2013 CE) were considered in the correlation analysis between the GV7-C ice core records and climate data. These periods were selected depending on the availability of the climate data (e.g., SAM index) and to ensure a large sample size. All datasets used in the correlation analysis were linearly detrended prior to analysis and the statistical significance of Pearson correlation coefficients was assessed using a two-tailed Student's *t*-test, and significance levels were verified using the corresponding *p*-values. Moreover, emphasis is placed on correlation magnitude, temporal persistence, and physical consistency. Smoothed time series (3- and 5-year running means) were used to highlight low-frequency coherence between variables. The SAM and ENSO are assumed to be factors that potentially affect Antarctic climate variability (Turner et al., 2009; Cohen et al., 2012; Pohl et al., 2021; Wille et al., 2021), and the SOI and Niño3.4 indices describe changes in the Pacific Ocean that influence the Southern Ocean and Antarctic continent (Meyerson et al., 2002; Bertler et al., 2004). ENSO teleconnections to Antarctica are transmitted through Rossby wave trains and associated circulation anomalies, which are seasonally modulated, while the IOD is typically phase-locked to austral winter/spring conditions. Similarly, SAM variability influences Antarctic climate through shifts in the westerly wind belt

and associated changes in storm tracks. Because the isotopic composition recorded in each annual ice-core layer represents the integrated snowfall accumulated throughout the year, the GV7-C record reflects the combined influence of seasonal processes. For this reason, climate data were initially examined at both annual (January to December) and seasonal (DJF, MAM, JJA, SON) scales to assess potential relationships with the GV7-C ice core data. Although some seasonal differences were observed, the overall patterns and physical interpretation remained consistent when annual means were used. Therefore, annual values were selected to represent the net integrated climate signal preserved in the ice core.

For the 1957–2013 CE period, the following climate indices were compared with the annual means of the GV7-C ice core records: station-based SAM index (Marshall G and National Center for Atmospheric Research Staff, 2018), the Southern Oscillation Index (SOI) (https://www.ncei.noaa.gov/access/monitoring/enso/soi), Niño3.4 index (https://psl.noaa.gov/gcoswgsp/Timeseries/Nino34), Indian Ocean Dipole (IOD) index representing the SST gradient between the western and southeastern equatorial IO (https://psl.noaa.gov/gcos_wgsp/Timeseries/DMI), SST anomaly in the southeastern IO (SST-SEIO) (https://psl.noaa.gov/gcos_wgsp/Timeseries/DMI), and reconstructed sea ice extent (SIE) over the Ross–Amundsen Sea sector (162°E–250°E) and the East Antarctic sector (71°E–162°E) (Fogt et al., 2023). Moreover, for the 1957–2013 CE period, spatial correlation analysis (at 95% confidence interval) was conducted between annual GV7-C records and gridded ERA5 reanalysis data (air temperature, SST, sea ice concentration [SIC], 10-m wind speed, zonal [u] and meridional [v] wind components, and total precipitable water) using Climate Reanalyzer developed by the University of Maine, USA (https://climatereanalyzer.org/). Since ice-core isotopic signals reflect a broad range of thermodynamic and dynamic influences, spatial correlation analyses were conducted for physically plausible scenarios to help identify potential moisture supply regions over a longer time period (1957–2013 CE) than previous studies (Caiazzo et al., 2017; Khan, 2019). Spatially coherent and physically interpretable patterns are selectively presented and used as supportive evidence in the interpretation of climate-related signals from the GV7-C ice core. Principal component analysis (PCA), a linear dimensionality reduction technique, was employed to investigate potential similarities in variability between the annual means of the ice-core records and seasonal and annual means of climate datasets (IOD, SST-SEIO, SAM, SOI, Niño3.4, SIE) for 1957–2013 CE. The PCA results conducted on annual mean values were selected and presented in this study. For the 1872–2013 CE period, the GV7-C ice core data were compared with the IOD index, SST-SEIO, reconstructed SST anomaly over the Southern Hemisphere (https://www.ncei.noaa.gov/access/monitoring/climate-at-a-glance/global/time-

series) (Huang et al., 2017), reconstructed SAM index (https://psl.noaa.gov/data/20thC_Rean/timeseries/monthly/SAM), and Niño3.4."

- Limited or no consideration of the physical mechanisms for how climate variability modes influence Antarctic weather and climate and how that is reflected in the method.

    1. For example, for ENSO if the annual period used is January to December (not specified in the manuscript), this splits ENSO events in half (which usually run from austral winter through to late austral summer) and is not related to the physical process that links ENSO variability to the Antarctic climate via Rossby wave train, and how this interacts with the phase of SAM and in different seasons.
    2. Considerations required for IOD include phase lock (e.g. the influence of IOD on southern hemisphere climate is phase locked by the arrival of the southern monsoon in the southern hemisphere and is usually only active between austral winter and early summer) and the seasons when the Rossby wave teleconnection to Antarctic climate is possible and not reflected by the interactions with the polar jet.
    3. SAM considerations – asymmetric vs symmetric component, and how SAM interacts with weather systems in the region that influence ice core interpretation.

Answer: Thank you for the helpful comment. Since the ice core signals reflect broad range of processes, with the GV7-C ice core data (one of the high SA, well-dated, high-resolution data), we have considered both annual and seasonal characteristics of the climate modes, and tested the analysis (correlation, PCA analysis) on multiple cases (can be said many) at initial steps. We tested seasonal values and found no significant deviations when using annual values instead of seasonal values, we then selected annual values. We have mentioned "Jan to Dec" for annual period in the materials and method section.

We agree on the importance regarding the physical mechanisms linking large-scale climate modes to Antarctic climate variability. ENSO, IOD, and SAM exhibit strong seasonal characteristics and influence Antarctic climate through seasonally dependent dynamical pathways. Because ice-core isotopic records represent the integrated precipitation signal accumulated throughout the year, the annual layer reflects the combined influence of seasonal processes rather than a single seasonal state. For this reason, we initially tested both seasonal (DJF, MAM, JJA, and SON) and annual correlations in the exploratory phase of the analysis. While some seasonal differences were observed, the overall patterns of association and physical interpretation remained consistent when annual means were used. Therefore,

annual (January to December) values were selected to represent the net integrated climate signal recorded in the GV7-C ice core.

We acknowledge that ENSO events often span austral winter through late austral summer and that IOD variability is phase-locked to austral winter–spring conditions. However, because the isotopic composition recorded in each annual layer reflects snowfall accumulated across multiple seasons, annual averaging is appropriate for capturing the integrated teleconnection signal.

To clarify this methodological reasoning, we have stated in Section 2.3 that climate data were examined on both annual (January to December) and seasonal (DJF, MAM, JJA, SON) scales prior to selecting the annual representation. This clarification has been added to improve transparency regarding the physical interpretation underlying the methodological design.

Section 2: Materials and methods

"The $\delta^{18}O$ ($\delta^{18}O$ preferred and the correlation with δD is 0.99), *d*-excess, and SA from the GV7-C ice core were used in the analysis. Two time periods (1957–2013 CE and 1872–2013 CE) were considered in the correlation analysis between the GV7-C ice core records and climate data. These periods were selected depending on the availability of the climate data (e.g., SAM index) and to ensure a large sample size. All datasets used in the correlation analysis were linearly detrended prior to analysis and the statistical significance of Pearson correlation coefficients was assessed using a two-tailed Student's *t*-test, and significance levels were verified using the corresponding *p*-values. Because climatic and ice-core time series may exhibit serial autocorrelation, which can reduce the effective degrees of freedom and potentially inflate nominal significance levels, statistical results are interpreted carefully. Emphasis is placed on correlation magnitude, temporal persistence, and physical consistency rather than solely on nominal *p*-values. Smoothed time series (3- and 5-year running means) were used to highlight low-frequency coherence between variables. The SAM and ENSO are assumed to be factors that potentially affect Antarctic climate variability (Turner et al., 2009; Cohen et al., 2012; Pohl et al., 2021; Wille et al., 2021), and the SOI and Niño3.4 indices describe changes in the Pacific Ocean that influence the Southern Ocean and Antarctic continent (Meyerson et al., 2002; Bertler et al., 2004). ENSO teleconnections to Antarctica are transmitted through Rossby wave trains and associated circulation anomalies, which are seasonally modulated, while the IOD is typically phase-locked to austral winter/spring conditions. Similarly, SAM variability influences Antarctic climate through shifts in the westerly wind belt and associated changes in storm tracks. Because the isotopic composition recorded in each annual ice-core layer represents

the integrated snowfall accumulated throughout the year, the GV7-C record reflects the combined influence of seasonal processes. For this reason, climate data were initially examined at both annual (January to December) and seasonal (DJF, MAM, JJA, SON) scales to assess potential relationships with the GV7-C ice core data. Although some seasonal differences were observed, the overall patterns and physical interpretation remained consistent when annual means were used. Therefore, annual values were selected to represent the net integrated climate signal preserved in the ice core.

For the 1957–2013 CE period, the following climate indices were compared with the annual means of the GV7-C ice core records: station-based SAM index (Marshall G and National Center for Atmospheric Research Staff, 2018), the Southern Oscillation Index (SOI) (https://www.ncei.noaa.gov/access/monitoring/enso/soi), Niño3.4 index (https://psl.noaa.gov/gcoswgsp/Timeseries/Nino34), Indian Ocean Dipole (IOD) index representing the SST gradient between the western and southeastern equatorial IO (https://psl.noaa.gov/gcos_wgsp/Timeseries/DMI), SST anomaly in the southeastern IO (SST-SEIO) (https://psl.noaa.gov/gcos_wgsp/Timeseries/DMI), and reconstructed sea ice extent (SIE) over the Ross–Amundsen Sea sector (162°E–250°E) and the East Antarctic sector (71°E–162°E) (Fogt et al., 2023). Moreover, for the 1957–2013 CE period, spatial correlation analysis (at 95% confidence interval) was conducted between annual GV7-C records and gridded ERA5 reanalysis data (air temperature, SST, sea ice concentration [SIC], 10-m wind speed, zonal [u] and meridional [v] wind components, and total precipitable water) using Climate Reanalyzer developed by the University of Maine, USA (https://climatereanalyzer.org/). Since ice-core isotopic signals reflect a broad range of thermodynamic and dynamic influences, spatial correlation analyses were conducted for physically plausible scenarios to help identify potential moisture supply regions over a longer time period (1957–2013 CE) than previous studies (Caiazzo et al., 2017; Khan, 2019). Only spatially coherent and physically interpretable patterns are selectively presented and used as supportive evidence in the interpretation of climate-related signals from the GV7-C ice core. Principal component analysis (PCA), a linear dimensionality reduction technique, was employed to investigate potential similarities in variability between the annual means of the ice-core records and seasonal and annual means of climate datasets (IOD, SST-SEIO, SAM, SOI, Niño3.4, SIE) for 1957–2013 CE. The PCA results conducted on annual mean values were selected and presented in this study. For the 1872–2013 CE period, the GV7-C ice core data were compared with the IOD index, SST-SEIO, reconstructed SST anomaly over the Southern Hemisphere (https://www.ncei.noaa.gov/access/monitoring/climate-at-a-glance/global/time-series) (Huang et al., 2017), reconstructed SAM index (https://psl.noaa.gov/data/20thC_Rean/timeseries/monthly/SAM), and Niño3.4."

- Consideration of data reliability (e.g. ERA5 data reliability prior to 1979 in the Southern Hemisphere has been highlighted as having issues and artificial trends due to limited data prior to satellites). Reanalysis that considers only pressure (e.g. 20th century reanalysis) have been shown to be more reliable as they have less step changes in the number and type of observation used in data assimilation.

Answer: We appreciate the comment and agree on the careful consideration of reanalysis data. We acknowledge that the analysis included in this study was initiated and driven by previous studies at this site that mentioned the influences of climate indices (e.g., ENSO, SAM, SOI), but were based on relatively shorter records (mostly since 1979). We expanded the comparison with reanalysis data to test and obtain supporting confirmation from spatial correlations, since the ice core isotopic signals reflect a broad range of influencing factors. The purpose was to support the assumptions and identification of the moisture supply region from the perspective of spatial relevance over a relatively longer time period (1957–2013 CE) than previous studies (Caiazzo et al., 2017; Khan, 2019). The results were used as support in the interpretation based on the spatial correlation maps with ERA5 reanalysis. The identification of positive and negative correlations, the regions exhibiting these correlations, and the relevant seasons (where possible) were considered to support the interpretation; the interpretations are not based solely on ERA5 spatial correlation analysis. Within the scope of the study, we checked the spatial correlation maps, and we agree that it is possible and worthwhile to expand the data selection and analyses in greater detail (e.g., using 20th century analysis) in future studies. Alternative reanalysis products may offer complementary perspectives, and such comparisons represent a valuable direction for future research. We have revised Section 2.3 to explicitly state that spatial correlation analyses using ERA5 are used as supportive evidence and that interpretations are not based solely on reanalysis-derived fields.

"Since ice-core isotopic signals reflect a broad range of thermodynamic and dynamic influences, spatial correlation analyses were conducted for physically plausible scenarios to help identify potential moisture supply regions over a longer time period (1957–2013 CE) than previous studies (Caiazzo et al., 2017; Khan, 2019). Only spatially coherent and physically interpretable patterns are selectively presented and used as supportive evidence in the interpretation of climate-related signals from the GV7-C ice core."

Limited details provided on the principle component analysis method and results.

Answer: We thank for pointing out the need for clearer methodological detail regarding the principal component analysis. In response, we have expanded the description of the PCA procedure in Section 2.3 and clarified the interpretation of the results in Section 3.2.1.

Specifically, we now state that all variables included in the PCA were standardized to zero mean and unit variance prior to analysis to ensure comparability among datasets with different units and magnitudes. The PCA was conducted based on the correlation matrix, and components with eigenvalues greater than 1 were retained following the Kaiser criterion. No rotation was applied, as the objective was to identify the dominant modes of joint variability rather than to maximize separation between components.

In addition, we have revised Section 3.2.1 to clarify the physical interpretation of the principal components and to explicitly present the loading matrix (correlation coefficients at $p < 0.05$) in Table 5. The variance explained by each principal component and the cumulative variance are now clearly reported. The revised text emphasizes that PCA results are interpreted in terms of coherent thermodynamic and dynamic variability patterns rather than as evidence of direct causality. We believe these revisions improve the transparency and robustness of the PCA methodology and clarify how the results support the overall interpretation of climate-related signals in the GV7-C ice core.

To address this point, we expanded the PCA description in Sect. 2.3 and clarified the interpretation of the PCA loadings in Sect. 3.2.1. We also included SST-SEIO among the PCA variables to align with the correlation analysis for 1957–2013 CE. The revised text is provided below.

Section 2.3 Climate data and analysis: "Principal component analysis (PCA), a linear dimensionality reduction technique, was employed to investigate any potential similarities in the variation within the annual means of ice core records and seasonal and annual means of climate datasets (IOD, SST-SEIO, SAM, SOI, Niño3.4, SIE) for 1957–2013 CE). The PCA results conducted on annual mean values were selected, and presented in this study."

Section 3.2.1. Correlation with large-scale climate modes:

"PCA analysis conducted for 1957–2013 CE, with the loading matrix (correlation coefficients at $p < 0.05$) presented in Table 5. Principal component (PC) 1 clustered $\delta^{18}O$, the SAM, SOI, Niño3.4, and SIE over the East Antarctica and Ross-Amundsen Sea region. This reflected the importance of both thermodynamic and dynamic effects on the decrease (increase) in $\delta^{18}O$ with an increase (decrease) in the SIE,

stronger (weaker) westerly winds (i.e., the SAM and SOI), and lower (higher) SSTs in the Niño3.4 region. In PC 2, *d*-excess and SA were clustered with IOD, SAM, SIE, and particularly strong signal of SST-SEIO. This can represent the increasing (decreasing) *d*-excess with increased (decreased) evaporation with warm (cold) SSTs particularly over the southeastern IO. Moreover, there could be a weak relevance with enhanced (weakened) air mass transport with strong westerlies (i.e., the SAM), consequent wind-induced increase (decrease) in SIE over East Antarctica and relatively cooler temperature over the eastern IO (decreasing IOD). It is again ambiguous to explain the negative correlation observed between the SA and SST-SEIO in PC 2. However, PC 3 included SA only, with more stronger signals of IOD, SAM, SOI, Niño3.4 and SIE over the East Antarctica. This can represent the thermodynamic effects on SA with increased (decreased) evaporation with warm SSTs over western equatorial IO and central tropical PO (i.e., the SOI and Niño3.4), enhanced moisture transport with strong westerlies (i.e., the SAM), and the wind-induced SIE over East Antarctica. PC 4 was characterized by an increasing (decreasing) $\delta^{18}O$, *d*-excess with decreasing (increasing) SST-SEIO which can be explained by the intrusion of different air masses with evident *d*-excess signals together with $\delta^{18}O$. Overall, PCA classified the variables into species representing the climatic signals corresponding to the PO (PC 1) and southeastern IO sector of the Southern Ocean (PC 2). Interestingly, the relatively strong detectability of the thermodynamic effect on *d*-excess, which is induced by the IO sector, likely to indicate the significant (detectable) temperature signals in this region."

Table 5. Loadings of the variables for the first four principal components (PCs) of the PCA analysis conducted with the data for 1957–2013 CE. Larger values of correlation coefficients ($r > 0.3$, at $p < 0.05$) are marked in underlined bold.

Variables	PC1	PC2	PC3	PC4
SA	0.04	**–0.48**	**0.43**	–0.04
$\delta^{18}O$	**–0.39**	0.20	–0.04	**0.77**
d-excess	0.05	**0.63**	–0.07	**0.49**
IOD	0.12	**–0.30**	**0.77**	0.27
SST (SEIO)	–0.07	**0.82**	–0.08	**–0.40**
SAM	**0.52**	**0.30**	**0.56**	–0.08
SOI	**0.82**	–0.23	**–0.43**	0.13
Niño3.4	**–0.80**	0.27	**0.47**	–0.13
SIE (EA)	**0.52**	**0.31**	**0.38**	0.00
SIE (RA)	**0.84**	0.29	0.13	0.05
Variance explained (%)	*27*	*18*	*17*	*11*
Cumulative percent (%)	*27*	*45*	*62*	*73*

- Multiple correlations are calculated which increases the type-1 error (i.e. increased chance of false positives). How is this being considered?

Answer: We agree that conducting many correlation tests can increase the chance of false positives. In this revision, we clarify in Sect. 2.3 that correlations are interpreted conservatively, with emphasis on (i) effect size, (ii) temporal persistence, and (iii) physical consistency, rather than on isolated p-values. The correlation analyses were largely hypothesis-driven, motivated by prior work at GV7 and nearby sites, and the spatial correlation maps are used as supporting evidence to evaluate whether the inferred relationships are geographically coherent and physically plausible over 1957–2013 CE.

Comment 2: (2) Most of the figures are in the supplementary material. These are referred to in the results and essential to be able to understand the results and interpretation discussed so need to be made more concise to be able to be included in the main text.

Answer: Thank you for this clear comment. As we have changed the manuscript structure according to the other comments, the figures in the supplementary material were generated by the spatial correlation analysis with ERA5 reanalysis, as a supportive results to the main interpretations (section 3.2.1. and 3.3) of the manuscript. The description of the figures moved to section 3.2.2. (Spatial correlation analysis with ERA5 reanalysis), after the section 3.2.1. Correlation with large-scale climate modes (the correlation analysis, PCA analysis), to indicate its importance (supportive results) after section 3.2.1. We included information in materials and method section *(2.3. Climate data and analysis)*, as it shown below.

"Since ice-core isotopic signals reflect a broad range of thermodynamic and dynamic influences, spatial correlation analyses were conducted for physically plausible scenarios to help identify potential moisture supply regions over a longer time period (1957–2013 CE) than previous studies (Caiazzo et al., 2017; Khan, 2019). Only spatially coherent and physically interpretable patterns are selectively presented and used as supportive evidence in the interpretation of climate-related signals from the GV7-C ice core."

Moreover, we removed Supplementary Figures 9 and 10 because they described widely known relationships between climate variables and Niño 3.4 and SAM, rather than relationships specific to the GV7-C ice core.

We revised Sect. 3.2.2 (Spatial correlation analysis with ERA5 reanalysis) to improve clarity and to make the supporting figures more concise. The spatial-correlation results are now consolidated and presented as three combined figures in the

Supplement (Figs. S1–S3), which summarize the key, physically interpretable patterns used in our discussion. The revised text for Sect. 3.2.2 is provided below.

3.2.2. Spatial correlation analysis with ERA5 reanalysis

Spatial correlation analyses (95% confidence interval) were conducted between annual GV7-C records (δ18O, d-excess, and SA) and annual/seasonal ERA5 reanalysis fields for 1957–2013 CE to explore potential spatial patterns consistent with moisture supply and transport pathways. Significant and physically interpretable patterns are selectively presented in the Supplement (Figs. S1–S3) and are used as supporting evidence in the discussion of likely source regions. For interpretation, the Pacific Ocean (PO) sector is defined here as the western Pacific (90–160°E), Ross Sea (160°E–130°W), and Amundsen–Bellingshausen Seas (130–60°W), while the Indian Ocean (IO) sector is defined as 20–90°E.

Annual mean δ18O shows positive correlations with 2 m air temperature and SST primarily over the PO sector (Fig. S1a, b). Positive relationships with air temperature (2 m and 850 hPa) and total column precipitable water are most evident during DJF over parts of the PO and IO sectors (Fig. S1d–f). Negative correlations are observed with sea ice concentration (SIC) over the Ross Sea region (Fig. S1c). Wind-speed correlations (10 m; annual and MAM) are generally negative (Fig. S1g, j), and zonal wind (u-wind) correlations highlight the belt of strong westerlies (Fig. S1h, k). The meridional wind (v-wind) correlations suggest a northward flow signature from the western PO sector and a southward flow signature from the IO sector during DJF (Fig. S1i), whereas these patterns weaken in MAM (Fig. S1l). Overall, δ18O exhibits its clearest spatial coherence during DJF and MAM, consistent with the seasonality of transport and snowfall in this coastal sector (Delmotte et al., 2000; Caiazzo et al., 2017). These patterns provide qualitative support for a relatively stronger PO-sector influence on δ18O at GV7-C during DJF–MAM, although the overall relationships remain modest.

Annual mean d-excess exhibits positive correlations with air temperature (2 m and 850 hPa) over both the western PO and IO sectors (Fig. S2a–c). Temperature correlations in the IO sector are particularly evident in SON (Fig. S2c), whereas the d-excess response to temperature appears weaker in DJF (not shown). Correlations with SST (SON), SIC (JJA), and total column precipitable water (annual) further support a contribution of air masses from the IO sector and western PO to the GV7 region (Fig. S2d–f). In contrast to δ18O, correlations with wind speed and wind direction are relatively weak, except for a positive correlation with 10 m wind speed in some regions (Fig. S2g). The v-wind pattern indicates a southward flow signature from the IO sector and a northward flow signature in the western PO sector (Fig. S2i). Taken together, these spatial patterns suggest that thermodynamic source-region variability (e.g., SST/air-temperature conditions) may play a comparatively larger role for d-excess at GV7-C than do purely dynamical indicators, and they are

consistent with a potentially important contribution from the IO sector, particularly during SON.

No clear and temporally consistent relationships are observed between SA and the investigated climate variables; only weak and spatially limited patterns are identified (Fig. S3). For example, SA shows weak negative correlations with 2 m temperature over parts of the Amundsen Sea coast and weak positive correlations with total column precipitable water offshore of the Ross Sea coast (Fig. S3a, b). SA also shows weak negative correlations with SIC over the Ross Sea region (Fig. S3c). Wind-speed correlations (10 m and 850 hPa) are weakly positive over parts of the PO sector (Fig. S3d, g), and the associated u- and v-wind patterns suggest modest transport signals (Fig. S3e, f, h, i). Overall, these results indicate that SA at GV7-C is likely influenced by multiple factors, including synoptic variability and transport efficiency, which may mask simple relationships with large-scale indices at annual resolution.

In sum, the spatial correlation patterns suggest that GV7-C records reflect regional variability linked to both the PO and IO sectors. The δ18O correlations that are most evident during DJF and MAM motivate consideration of SAM-related dynamical influences during these seasons, while d-excess more strongly reflects thermodynamic variability linked to the IO sector, particularly during SON (Masson-Delmotte et al., 2003).

Supplementary data

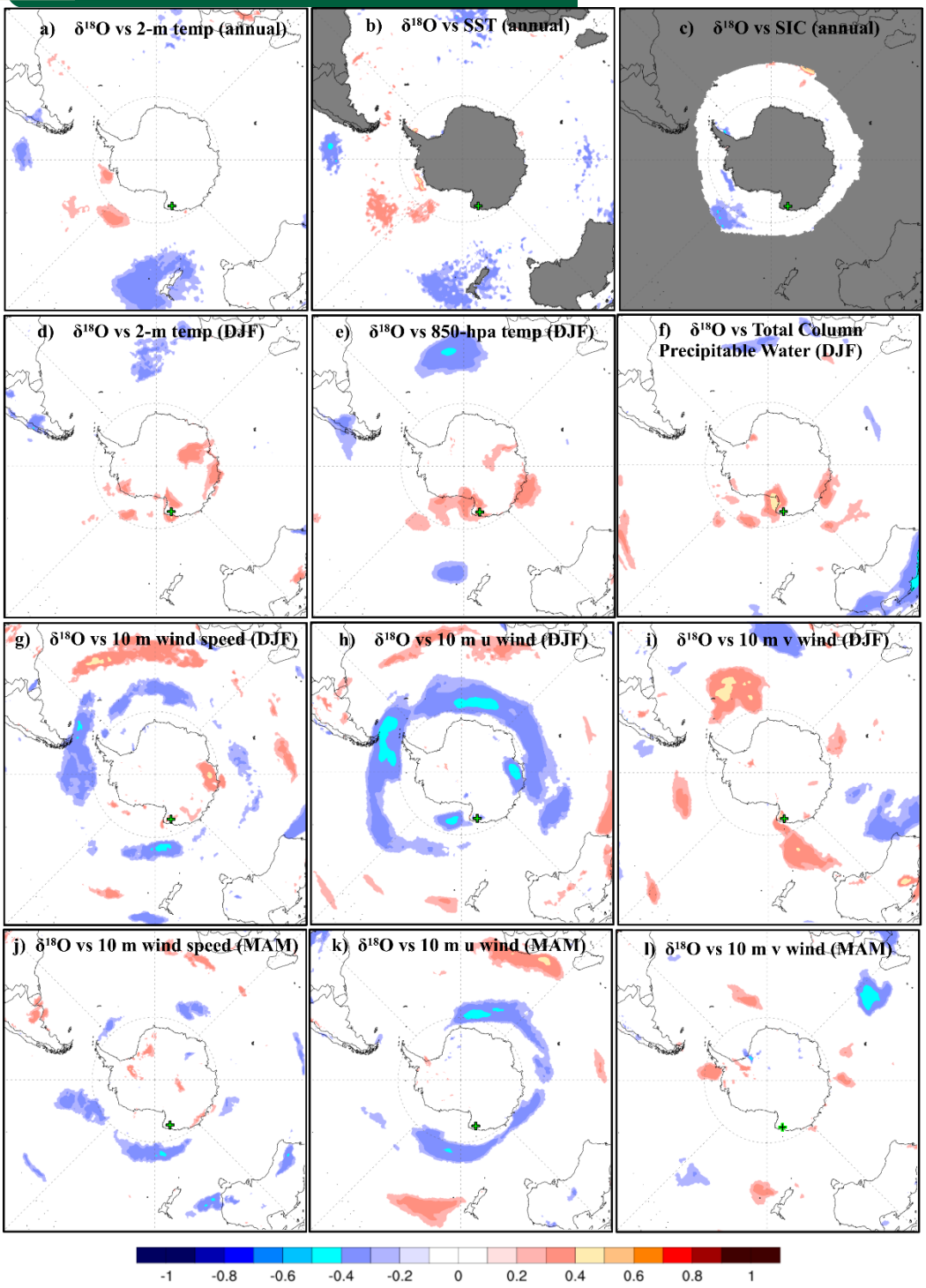

Figure S1. *Spatial correlation of $\delta^{18}O$ with (a, d, e) air temperature, (b) SST, and (c) SIC, (f) total column precipitable water, (g, j) wind speed, (h, k) u-wind components, and (i, l) v-wind components from the ERA5 reanalysis data for different seasons over the 1957–2013 CE period. The scale bars indicate Pearson's correlation coefficient (r) at $p < 0.05$. This figure was generated using Climate Reanalyzer (https://climatereanalyzer.org/) from the Climate Change Institute, University of Maine, USA.*

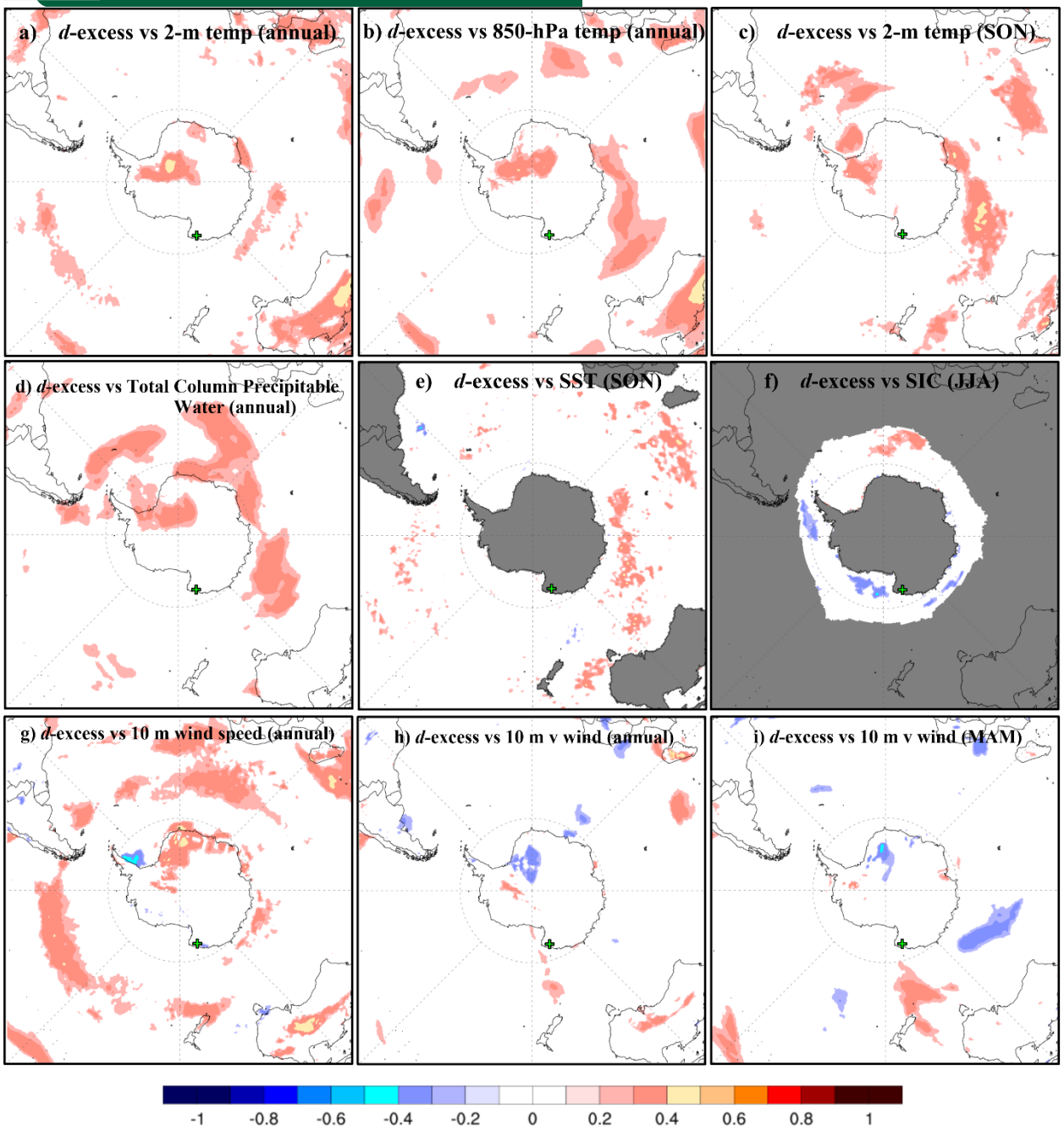

Figure S1. *Spatial correlation of d-excess with the (a, b, c) air temperature, (d) total column precipitable water, (e) SST, (f) SIC, (g) 10 m wind speed and (h, i) v-wind component from ERA5 reanalysis data for different seasons over the 1957–2013 CE period. The scale bars indicate Pearson's correlation coefficient (r) at $p < 0.05$. This figure was generated using Climate Reanalyzer (https://climatereanalyzer.org/) from the Climate Change Institute, University of Maine, USA.*

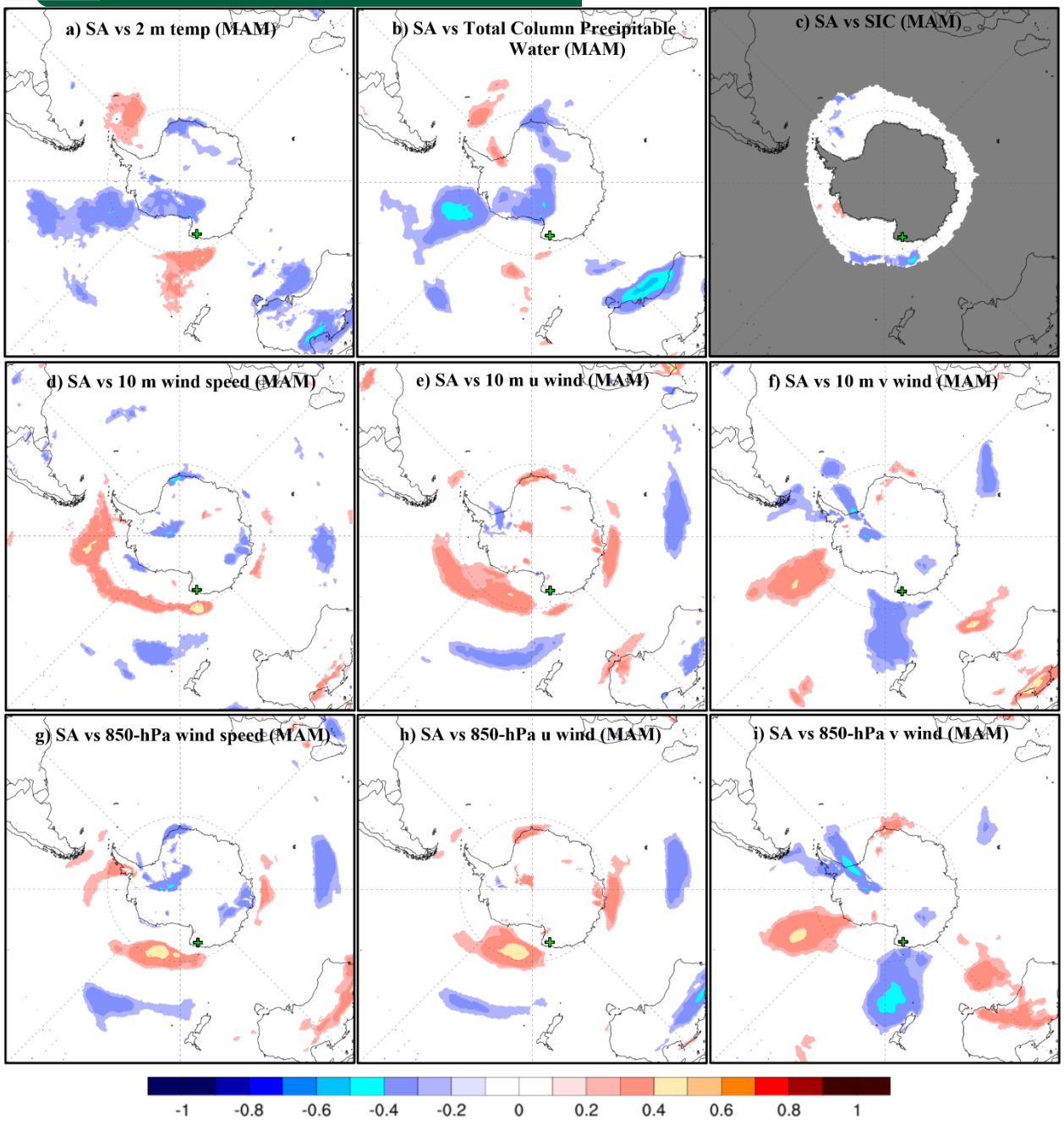

Figure S3. *Spatial correlation of SA with (a) air temperature, (b) total column precipitable water, (c) SIC, (d, g) 10 m wind speed, (e, h) u-wind components, and (f, i) v-wind components from ERA5 reanalysis data during the MAM season over the 1957–2013 CE period. The scale bars indicate Pearson's correlation coefficient (r) at p < 0.05. This figure was generated using Climate Reanalyzer (https://climatereanalyzer.org/) from the Climate Change Institute, University of Maine, USA.*

Comment 3: (3) Manuscript needs a major restructure. Currently there are a lot of discussion points in the results and it is challenging to determine what the key findings of the manuscript are. These need to be obvious based on the figures and results section, which is currently not the case with multiple figures in the supplementary and no clear structure to the result and discussion section.

Answer 3: Thank you for the clear comment that helped us to reconsider and re-organize the structure of the manuscript. We revised the structure of the manuscript. Duplications, unnecessary details in results, discussion, as well as in introducing sentences, have been edited (removed and edited concisely). We also edited/combined the interconnected results/duplicated but described separately as independent in the previous version. Results and discussion parts have been combined in one section (Section 3.), as shown in below.

Previous version	Edited version
3 Results 3.1 Characterization of the GV7-C ice core record 3.2 Relationship with climate variables during 1957–2013 3.2.1 Relationship with climate variables from ERA5 Reanalysis 3.2.2 Relationship with large-scale climate modes 3.3 Relationship with Long-Term Climate Modes 4 Discussion and implications	3 Results and discussion 3.1 Characterization of the GV7-C ice core record 3.2 Climate signals for the 1957–2013 CE period 3.2.1. Correlation with large-scale climate modes 3.2.2. Spatial correlation analysis with ERA5 reanalysis 3.3 Climate Signals for the Long-Term Records (1872–2013 CE) 3.4 Discussion and implications

We edited the captions of figures and tables, more clearly. We removed Supplementary Figures 9 and 10 because they described widely known relationships between climate variables and Niño 3.4 and SAM, rather than relationships specific to the GV7-C ice core.

We edited (removed duplications, re-organized the statements, highlighted key findings with supporting/relevant references) section 3.4 (Discussion and implications), abstract and conclusion, as it shown below.

"The variations in SA data from the GV7-C ice core show no obvious trend and are not correlated to climate drivers examined in this study. The SA of the GV7-C ice core is assumed to be affected by the coupled influence of dynamic processes (i.e., the transport pathways and transport efficiency of moist air) or abrupt synoptic events (e.g., intense transport by atmospheric river events) (Turner et al., 2019; Wille et al., 2021). The variability in SA is affected by moisture transport via large-scale atmospheric circulation (Thomas et al., 2008) and synoptic-scale short-lived events (e.g., atmospheric river events, atmospheric rivers) (Turner et al., 2019; Wille et al., 2021) and evident in the ice core records from coastal regions (Servettaz et al., 2020; Jackson et al., 2023). Moreover, the intensity and frequency of cyclone events also affect snowfall in Antarctic coastal areas (Dalaiden et al., 2020a). Particularly, in the Ross Sea region, the cyclonically driven SA is dominant and the region is sensitive

to tropical and local climate drivers (Bertler et al., 2018). The contribution of synoptic-scale transport has been reported to be large for Victoria Land based on simulations over the 1985–2014 period (Dalaiden et al., 2020a). The influence of the ENSO on SA was evident at the Law Dome site (Roberts et al., 2015).

Based on the correlation of $\delta^{18}O$ in the GV7-C ice core with Nino 3.4, SOI, SAM, and SIE over the Ross-Amundsen Sea sector for 1957–2013 CE, the increasing (decreasing) $\delta^{18}O$ can be partly explained by the intrusion of relatively warm (colder) and moist (dry) air mass mainly through the PO sector of the Southern Ocean. This finding is comparable to other ice cores from the coastal Antarctica. In the Aurora Basin North ice core from East Antarctica, a weak negative correlation ($r = –0.24$) was observed between the SAM and $\delta^{18}O$ for 2005–2014 CE (Servettaz et al., 2020). This suggests a negative phase of the SAM channeled the intrusion of warm and moist air inland, consequently causing an increase in $\delta^{18}O$ at this site. Moreover, large precipitation events were influential on $\delta^{18}O$ signal, and further suggested as a tracer of atmospheric circulation. In the Mount Brown South ice core in East Antarctica, evidence for moisture transport from the southern IO has been detectable from $\delta^{18}O$ signal, and the extreme precipitation events are linked with high-pressure systems in the mid-latitudes which increase the transport of warm and moist air mass from the southern IO (Jackson et al., 2023). In another ice core from Adélie Land covering the 1946–2006 CE period, decadal variations in $\delta^{18}O$ and regional temperature were correlated (Goursaud et al., 2017). Moreover, $\delta^{18}O$ shows a tendency to decrease with increasing wind speed. However, the $\delta^{18}O$ on an annual scale could not be explained by changes in the SIE and temperature, indicating the importance of site-dependent climate signals in coastal ice cores (Goursaud et al., 2017). In another study, isotope-based results indicated colder SSTs, a higher SIE, stronger katabatic winds, and decreasing SA in the Victoria Low Glacier ice core during the 1288–1807 period (the Little Ice Age period) (Bertler et al., 2011). Little Ice Age-related cooling is also evident in the $\delta^{18}O$ signal from the Hercules Neve ice core for the 1770–1890 period (Stenni et al., 1999) and frequent cold intervals in the Talos Dome ice core (Stenni et al., 2002). In line with these observations, a slight decreasing trend was observed in the $\delta^{18}O$ signal from the GV7-C ice core during the 1782–1845 CE period (Fig. 4), which may be part of Little Ice Age cooling. After 1845, there was no long-term trend in $\delta^{18}O$ from the GV7-C ice core; rather, values lower than the long-term mean were frequently observed (the blue lines in Fig. 4). This depletion of $\delta^{18}O$ observed from the GV7-C ice core may be possibly linked with changes in atmospheric circulation (e.g., SAM-related cooling) (Thompson and Solomon, 2002). Moreover, in terms of temperature reconstruction, $\delta^{18}O$ signal in the GV7-C ice core is contrast to anthropogenic global warming, suggesting more local/regional variations or various climatic factors.

Based on the correlation of d-excess with SST-SEIO and SST anomaly (Tables 4 and 6), the d-excess signal from the GV7-C ice core likely to preserve the

thermodynamic changes (i.e., SST changes) particularly over the IO sector of the Southern Ocean. Notably, the southern Indian Ocean exhibits the most intense cyclonic activity in the Southern Ocean, which may enhance the detectability of this signal in the d-excess record (Simmonds et al., 2003). D-excess as an indicator of climate conditions in the source region (Jouzel et al., 1982; Sodemann and Stohl, 2009; Lewis et al., 2013), warming over the Southern Ocean, was found to co-vary with higher d-excess in the Victoria Lower Glacier ice core during the 1991–2000 CE period (Bertler et al., 2011). At the Law Dome ice core site, d-excess also reflects SST changes over the southern IO sector (Masson-Delmotte et al., 2003). Particularly the abrupt increase in the d-excess in the 1970s was consistent with the GV7-C ice core result. This relevance was explained by the abrupt changes in meridional atmospheric circulation, which led to the intrusion of warm subtropical moisture sources to the Antarctic coast during the 1970s (Masson-Delmotte et al., 2003). Changes in the SAM have also been linked to tropical SST changes and other tropical variabilities (Clem and Fogt, 2013; Ding et al., 2012). The climate signals in some coastal sites, including RICE, Mt. Erebus Saddle, and Styx Glacier, have been thought to be primarily indicative of local and regional conditions in the Ross Sea region (Rhodes et al., 2012, Nyamgerel et al., 2020, 2024). Similarly, the influence IOD on the eastern East Antarctic precipitation was more dominant than the SAM-induced changes for the 1979–2014 (Lee and Jin, 2024). The IOD-related variation in the precipitation is explained by waves originating from the Indian Ocean that propagate southeastward, and inducing a low-pressure anomaly near eastern east Antarctica, consequently reducing precipitation. Thus, in the GV7-C ice core site, variabilities linked to the SAM and remote teleconnections with SST over the IO sector of the Southern Ocean were assumed to be associated with d-excess.

Based on various correlation analysis with the climate variables used in this study, the following interpretations are summarized. During the period 1957–2013 CE, the correlation patterns based on $\delta^{18}O$ and *d*-excess support that snow precipitating at the GV7-C site mainly originates from the Southern Ocean possibly via western PO and southeastern Indian Ocean. For the longer time scale (1872–2013), the correlation patterns based on *d*-excess for SST indicates air mass from the Southern Ocean possibly via the Indian Ocean sector. This suggests a warmer (colder) ocean surface condition would be preserved in higher (lower) $\delta^{18}O$ (recent period) and *d*-excess values (recent and longer period) in the GV7-C ice core.

Lastly, it is notable that the importance of the GV7-C ice core records in climate studies. The historical temperature variability over the tropical ocean is important for global warming scenarios (IPCC, 2019). The projections show oceanic and atmospheric warming (Timmermann and Hellmer, 2013), and heat transported by the Southern Ocean further induces the melting of Antarctic ice shelves (Rignot et al., 2019). Particularly, the IO is experiencing the strongest and most robust warming (Du and Xie, 2008; Beal et al., 2019), largely driven by anthropogenic forcing (Dong

et al., 2014), and it is projected to warm non-uniformly (Sharma et al., 2023). The IO and the PO temperature anomaly affects the surface air temperature of Antarctica (Zhang and Duan, 2023). Moreover, warm SSTs in the western tropical IO excite a poleward-moving Rossby wave, inducing the changes in sea ice extent (Zhang et al., 2024). The coastal and inland Antarctic regions emerge an anomalous retreat of sea ice extent and warming due to the short-term significant intrusion of warm and moist air masses associated with strong negative phase of SAM (Ionita et al., 2018). The SAM variation in the recent period is unprecedented in the last millennia (Fogt and Marshall, 2020) and the increasing influence of the SAM-ENSO coupling has been reported since the 1940s (in coastal Dronning Maud Land) (Ejaz et al., 2022). Thus, understanding the response of the Antarctic climate to ocean variability of the IO sector would be important. Although, taking into account all possible influences was not feasible and would be beyond the scope of this study; nevertheless, the results may be useful for further research on the influence of atmospheric circulation, transport efficiency, and abrupt synoptic events in more details."

Abstract.

Polar ice cores are a valuable record of past climate variabilities, though the interpretation of these records and the climate of East Antarctica remains challenging due to the overlapping influences of diverse meteorological factors. This study investigates climate-related signals preserved in the GV7-C ice core from East Antarctica (1782–2013 CE), analyzing water isotopes ($\delta^{18}O$ and d-excess) and snow accumulation with comparison to various climate indices. Snow accumulation showed weak and inconsistent correlations with climatic variables, suggesting multiple influencing factors. δ18O correlations likely to indicates the detectability of climatic signals over the Pacific Ocean, while the d-excess corresponded to the Indian Ocean sector, for the 1957–2013 CE. Over the longer period (1872–2013 CE), $\delta^{18}O$ correlations weakened, suggesting shifting climatic influences, whereas d-excess retained correlations, emphasizing its reliability for tracking moisture-source. Notably, imprint of the temperature changes over the Indian Ocean on d-excess was relatively clear. The results highlight the potential teleconnections between Antarctic climate and tropical ocean conditions. Although, not all possible influences could be considered the scope of this study, the results may be useful for further research on the influence of atmospheric circulation, transport efficiency, and abrupt synoptic events.

4 Conclusions

The $\delta^{18}O$, *d*-excess, and SA data from the GV7-C ice core in East Antarctica for the 1782–2014 CE period were studied to identify potential correlations with various climate variables. Snow accumulation data were not strongly correlated climate drivers examined in this study, probably due to various influencing factors, while $\delta^{18}O$ and *d*-excess exhibited correlations with climate indices including Niño3.4, SOI, SAM, and SIE (Ross-Amundsen Sea sector) for the 1957–2013 CE. Notably, the *d*-excess show a persistent correlation with SST changes particularly over the southern IO sector. In the long-term records (1872–2013 CE), the correlation of $\delta^{18}O$ with the climate variables weakened, suggesting a shift in the climatic signals. In contrast, *d*-excess maintained the correlation with SST changes (IOD, SST-SEIO, SST anomaly) as well as with SAM. Correlation patterns based on $\delta^{18}O$ and *d*-excess suggest that moisture reaching the GV7-C site primarily originated from the Southern Ocean, potentially via the western Pacific and southeastern Indian Ocean for the 1957–2013 CE. However, this relevance appears to differ when considering the longer period (1872–2013 CE). Notably, relatively clear imprint of the SST changes over the IO sector on *d*-excess, likely to indicate the significant (detectable) temperature variations in this region. Overall, this study provides potential insights into teleconnections with low-latitude climate, in longer time periods, possibly over the Indian Ocean sector of the Southern Ocean, which is important in the context of global warming. Although, taking into account all possible influences were not feasible and would be beyond the scope of this study, the results may be useful for further research on the influence of atmospheric circulation, transport efficiency, and abrupt synoptic events in more details.

Comment 4: (4) Missing key relevant references. One example is around the studies that investigate the link between weather regimes (including atmospheric rivers) and their links to modes of climate variability in the region, and how these influence the interpretation of climate signals in ice cores. Some relevant examples are:

- Synoptic Weather Types for the Ross Sea Region, Antarctica in: Journal of Climate Volume 26 Issue 2 (2013),
- Links between Large-Scale Modes of Climate Variability and Synoptic Weather Patterns in the Southern Indian Ocean in: Journal of Climate Volume 34 Issue 3 (2021),
- Relationship Between Weather Regimes and Atmospheric Rivers in East Antarctica - Pohl - 2021 - Journal of Geophysical Research: Atmospheres - Wiley Online Library,
- Antarctic Atmospheric River Climatology and Precipitation Impacts - Wille - 2021 - Journal of Geophysical Research: Atmospheres - Wiley Online Library

- The Dominant Role of Extreme Precipitation Events in Antarctic Snowfall Variability - Turner - 2019 - Geophysical Research Letters - Wiley Online Library

Given the above, I recommend major revisions to strengthen the methodological transparency, clarify results and make the figures more concise and related to the key messages of the paper, and restructure to improve the interpretation and integration of findings within the broader Antarctic climate variability research.

Answer: Thank you for the clear suggestion, we have referred, and cited in relevant sections of the manuscript.

2.3 Climate data and analysis

The $\delta^{18}O$ ($\delta^{18}O$ preferred and the correlation to δD is 0.99), *d*-excess, and SA from the GV7-C ice core were used in the analysis. Two time periods (1957–2013 CE and 1872–2013 CE) were considered in the correlation analysis between the GV7-C ice core and climate data. These periods were selected depending on the availability of the climate data (e.g., SAM index) and to ensure a large sample size. All data in the correlation analysis were detrended and the significance of the analysis assessed by a two-tailed student's t-test, and the significance of Pearson correlation coefficients was verified using the *p*-values. The SAM and ENSO are assumed to be factors that potentially affect the Antarctic climate (Turner et al., 2009; Cohen et al., 2012; Pohl et al., 2021; Wille et al., 2021) and the SOI and Niño3.4 indices describe changes in the PO that affect the climate over the Southern Ocean and Antarctic continent (Meyerson et al., 2002, Bertler et al., 2004). For this reason, for the 1957–2013 CE period, following climate indices were compared with the annual means of GV7-C ice core records; station-

3.4 Discussion and implications

The variations in SA data from the GV7-C ice core show no obvious trend and are not correlated to climate drivers examined in this study. The SA of the GV7-C ice core is assumed to be affected by the coupled influence of dynamic processes (i.e., the transport pathways and transport efficiency of moist air) or abrupt synoptic events (e.g., intense transport by atmospheric river events). The variability in SA is affected by moisture transport via large-scale atmospheric circulation (Thomas et al., 2008; Udy et al., 2021; Cohen et al., 2012) and synoptic-scale short-lived events (e.g., atmospheric river events, atmospheric rivers) (Turner et al., 2019; Wille et al., 2021) and evident in the ice core records from coastal regions (Servettaz et al., 2020; Jackson et al., 2023). Moreover, the intensity and frequency of cyclone events also affect snowfall in Antarctic coastal areas (Dalaiden et al., 2020a). Particularly, in the Ross Sea region, the cyclonically driven SA is dominant and the region is sensitive to tropical

We appreciate all comments and suggestions on our manuscript. We are looking forward to its publication. Thank you for handling our manuscript and your patience.

Sincerely,
Jeonghoon Lee